Effects of topology on the controllability of brain connectomes through sparsity promoting control

Jethro Lim¹, Ilias Mitrai², Prodromos Daoutidis³, Catherine Stamoulis^{1,4}

Abstract—The fundamental mechanisms underlying the brain's ability to switch between dynamic (or physiological) states in response to cognitive demands are elusive, and have not been systematically correlated with the topology of neural circuits, especially in underdeveloped brains. We used a sparsity promoting closed-loop control framework, large datasets of resting-state connectomes from early adolescents and synthetic graphs, to investigate the role of graph topology on regional (node) controllability and control action on the connectome. Feedback costs were examined in ranges corresponding to nodes becoming self-controlled, losing their control action, or remaining self-controlled. Their associations with node connectedness and strength, and network modularity, fragility and resilience were assessed. Highly connected and central to the network nodes became self-controlled and maintained their control action on the network under high feedback cost, suggesting that brain regions with such properties may play critical roles in the connectome's controllabity. In addition, nodes in more modular, fragile and less resilient networks were self-controlled under overall higher feedback costs.

I. INTRODUCTION

Anatomical and functional neural circuits (the connectome) have topological characteristics that develop over the first two decades of life, and play a critical role in cognitive function across the lifespan [1], [2], [3], [4], [5], [6]. Their relationship with mechanisms that control dynamic changes in brain activity remain incompletely understood. However, cognitive function critically depends on the brain's ability to switch between dynamic, physiological and connectomic states. Thus, there is an unmet need to elucidate the relationships between the brain's topological characteristics and mechanisms underlying the controllability of its dynamics, especially during development, when both the connectome and neurodynamics undergo profound changes, as a result of synaptic pruning and changes in the balance between lowand high-frequency oscillatory activity [7], [8].

Prior work on brain controllability has used an openloop control framework applied primarily to structural networks [9], [10], has identified associations between structural characteristics of anatomical networks and control energy [9], [10], [11]. Studies on functional networks have correlated connectivity of large networks, e.g. the Default Mode Network (DMN), and/or highly connected regions (hubs),

This work was supported by the National Science Foundation, Awards 2207733 and 2207699

with controllability [12]. Most control studies on functional networks have focused on populations with neurological and/or neuropsychiatric disorders [12], [13], [14].

Only a few studies on the controllability of connectome dynamics have used a closed-loop control framework, although it has been used extensively in motor control, neurofeedback and brain-machine interface contexts [15], [16], [17], [18]. This framework is particularly well-suited for elucidating control actions of brain regions on each other, and assessing their relationships with key features of brain networks. In contrast to the open-loop framework, the closedloop approach can also account for the cost associated with the communication between regions. Studying controllability using this framework can provide fundamental mechanistic insights into the role of individual regions that are critical to the organization of the connectome but also controlbrain dynamics, and ultimately cognitive function. It can also identify potential regions that can be targeted by interventions, e.g., neurostimulation, to improve functional outcomes.

In incompletely maturated connectomes that have not yet attained their optimal topological configuration, controllability of their dynamics is elusive. Prior work on structural networks has shown that the optimization of dynamic network control is a developmental process [10]. Our recent work has used a sparsity-promoting closed-loop control framework to study the controllability of the early adolescent restingstate connectome [23]. In a small cohort, it showed that under high feedback cost, the connectome is controlled by a small set of (driver) regions that exert their control action on the rest of the brain. In this study, controllability of brain regions and their control action on each other, reflected in feedback control costs, and its relationships with regional and network-wide topological properties were investigated using resting-state fMRI data from early adolescents, and data-driven simulations. Given the inherent heterogeneity of developing brains and connectome variability, synthetic datasets were generated in order to study this problem in graphs with known topologies and constrained parameters.

II. MATERIALS AND METHODS

All analyses were conducted in the Harvard Medical School High Performance Cluster, using the software MAT-LAB (release R2023a, Mathworks, Inc) and publicly available python codes for synthetic graph generation. Topological analyses of all graphs used the custom-built Next-Generation Neural Data Analysis (NGNDA) platform [20].

Dept of Pediatrics, Boston Children's Hospital, Boston, MA, USA

² McKetta Dept of Chemical Engineering, Univ. of Texas Austin, Austin, TX, USA

³ Dept of Chemical Engineering and Materials Science, Univ. of Minnesota, Minneapolis, MN, USA

⁴Dept of Pediatrics, Harvard Medical School, Boston, MA, USA

A. Real datasets

Resting-state functional MRI (rs-fMRI) data from n = 500youth (median age = 121.0 months (Inter-Quartile Range (IQR) = 13.0, 54.4% girls), randomly selected from the Adolescent Brain Cognitive Development (ABCD) cohort [19] were analyzed. The data were preprocessed to account for motion and other artifacts, denoise and harmonize signals across multiple 3T acquisition systems, and reduce their dimension to 90 regions, to allow tractable control analyses. From each participant, their best-quality (with the lowest number of frames censored for motion) rs-fMRI run was used for analysis. Connectivity matrices were estimated using peak cross-correlation as a measure of connection strength. Corresponding adjacency matrices were estimated via thresholding, using a cohort-wide threshold equal to the boostrapped 75^{th} percentile of edge weights [21]. This eliminated weak and/or spurious edges. Topological properties were estimated from adjacency matrices, using tools in the NGNDA, and included community structure (modularity), network-wide median connectivity and region-specific connectedness (degree), regional importance in the network (eigenvector centrality), overall network strength (normalized sum of all edge weights, natural connectivity - a proxy for network resilience [25], and fragility [24]. Statistics for median connectivity (median = 0.43 (0.02)) and node degree (median = 5 (7), \sim 6% of all nodes) were also used to inform the parameter selection in synthetic graphs.

B. Synthetic graphs

1) Graphs with defined topologies: The Lancichinetti Fortunato Radicchi (LFR) algorithm was used to generate graphs with 200 nodes and data-derived properties [22]. Inputs to the model included node degree and community size (described by power law distributions), average degree, and parameter μ , which determines the proportion of edges between communities. Thus, a low μ reflects higher withincommunity edges and sparse connections between communities, a topological characteristic of developed brains. Figure 1 shows how μ influences the detectability of communities.

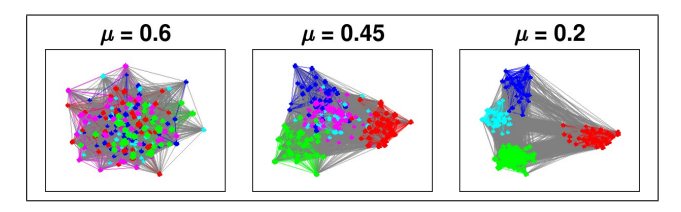


Fig. 1. Graph topology as a function of varying parameter μ (keeping average node degree constant). Node color reflects community membership.

To improve similarity between synthetic and real graphs (which were relatively sparse following thresholding), synthetic graphs with nodes connected to >50% of all nodes, and with other topological parameters far outside the range of real graph parameters, were excluded from further analysis. Furthermore, the LFR algorithm imposes a minimum node degree for convergence, while there is no such minimum in the real data. This leads to mismatch in their respective

degree distributions. To minimize this difference, synthetic graphs with degrees >20, i.e., >10% of possible connections) were also excluded. In the remaining graphs, each edge was assigned a weight, drawn from a normal distribution, in the range [0, 1]. The final dataset included 803 graphs with median degree = 19 (4), i.e., \sim 10% of all nodes, density <30% and median edge weight >0.4.

2) Graphs with random topologies: Random graphs with 200 nodes were generated using the Erdos-Renyi model. The input to the model was the probability of an edge existing in the graph, and was selected empirically in the range [0.1, 0.8], to avoid generating fully connected or disconnected graphs. Edges were randomly assigned based this probability, resulting in binary graphs with variable density. Edge weights were drawn from a normal distribution and that of the real data, in the range [0,1], and were randomly assigned to edges in each graph. Density and weights were then constrained in the same way as in the LFR graphs, to maximize the graphs' statistical similarity to the real ones. A total of 469 random graphs (median degree = 16 (13), 8% of all nodes) were selected for further analysis.

C. Closed-Loop Control Framework

The sparsity-promoting controller used in this study is described in detail in [23]. Briefly, for a linear dynamical system with state x and input u, we consider a controller u=-Kx, where K is the feedback gain matrix. The controller is designed (i.e., K is chosen) so that we optimize control performance, while at the same time penalizing its nonzero entries to account for the cost of feedback through a parameter p. In this study the control problem was solved for $p \in [10^{-4}, 30]$, and the elements of K were examined as a function of increasing feedback cost p.

III. RESULTS

Associations between feedback cost p and graph properties were investigated at two spatial scales, node and graph, and three ranges of p. The first range corresponds to values at which each node in the networks become self-controlled, i.e. K becomes diagonal. In the datasets, this range was [0.01, 0.51] for real, [0.01, 0.64] for LFR, and [0.01, 0.21] for random graphs. The second range corresponds to values for which a node no longer exerts a control action on the network, despite its connections to other nodes. The lower limit of this range corresponds to the first p value at which the diagonal K matrix becomes sub-diagonal (i.e., some of its entries become 0). In theory, the upper limit is when K becomes a zero matrix, but in this study it was restricted to p = 30.0. The median lower limit was 8.58 (0.07) for real, 8.98 (0.15) for LFR, and 8.84 (0.11) for random graphs. The third range corresponds to the 90^{th} percentile of p, at which a small subset of nodes remain self-controlled and exert a control action under very high feedback cost. The median of these values was 11.0 (0.96) for real, 11.3 (1.0) for LFR, and 10.6 (0.59) for random graphs.

A. Impact of regional (node) topology on feedback cost

Feedback cost associated with each node becoming self-controlled was examined as a function of its degree, strength and centrality. Real and synthetic graphs had a different number of nodes. Thus, degree and strength were normalized by node number and maximum strength, for the graphs to be comparable. Scatter plots in Figure 2 show this feedback cost as a function of these properties. Higher feedback costs were associated with higher node degree and centrality, in both real and LFR graphs. Similar positive associations were estimated for node strength, but only in real graphs. In random graphs, centrality was positively associated with feedback cost, but inversely associated with degree.

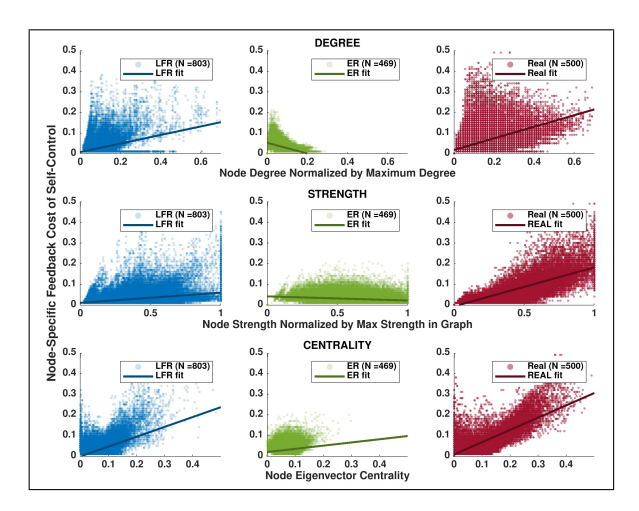


Fig. 2. Feedback costs at which nodes become self-controlled as a function of their topological properties.

These relationships were then examined for feedback costs when nodes lose their control action, and are shown in Figure 3. Higher costs correlated with higher node degree, centrality and strength across types of graphs, although the relationships were less clear (and nonlinear) for centrality. For both ranges of feedback costs, and across graphs, there was significant variability in the relationships between feedback cost at which transitions occur and node properties.

B. Impact of graph topology on feedback cost

Median (over all nodes) feedback cost \tilde{p} was examined as a function of graph modularity, natural connectivity, and fragility. To control for confounding effects of node strength, all properties were normalized by median graph strength.

Relationships between costs \tilde{p} at which nodes becoming self-controlled and graph properties are shown in Figure 4. Higher graph modularity was associated with higher \tilde{p} , although this relationship was not clear in real graphs. Similar associations were estimated for fragility. Lower natural connectivity was associated with lower \tilde{p} across graphs.

Associations between costs \tilde{p} at which nodes lose their control action and graph properties are shown in Figure 5. Across graphs, \tilde{p} was associated with lower modularity, natural connectivity and fragility across all graph types (although there was no clear relationship between modularity and \tilde{p} in

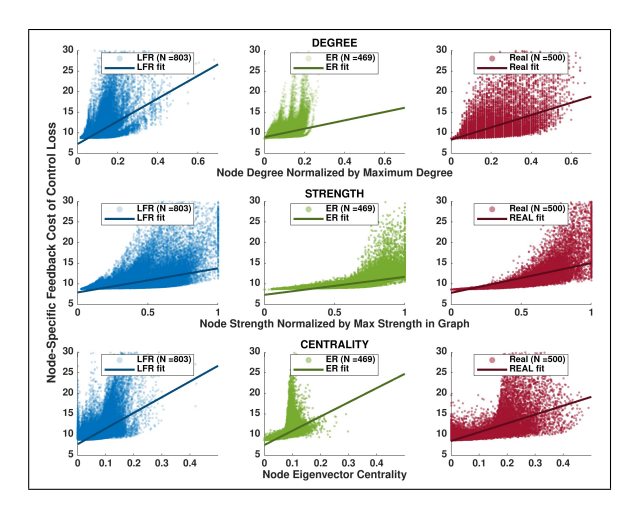


Fig. 3. Feedback costs at which nodes lose their control action as a function of their topological properties.

random graphs). Similar relationships were estimated for \tilde{p} at the 90th percentile, and are shown in Figure 6.

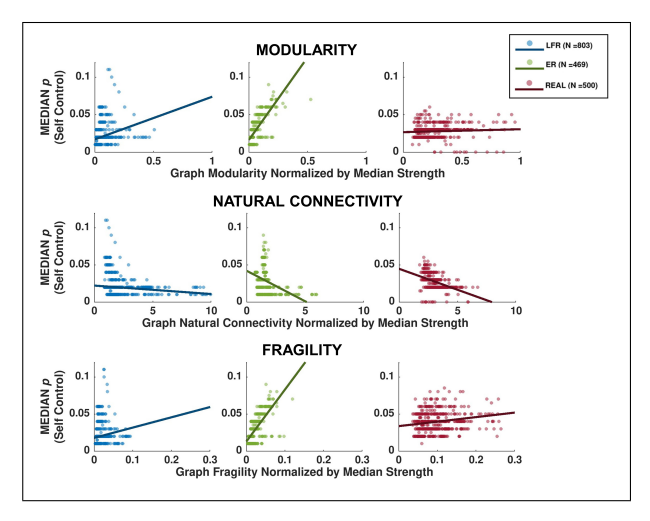


Fig. 4. Association between graph properties and median feedback cost at which nodes become self-controlled.

IV. CONCLUSIONS

We have investigated relationships between network controllability (within the lens of sparsity promoting control), a fundamental mechanism of neurodynamic regulation, and connectome topology. Identified positive associations between feedback costs and node degree, centrality and strength, suggest that topologically important and highly and strongly connected regions, such as hubs, become selfcontrolled and maintain their control action under high feedback cost. Functional hubs in the developing brain emerge over time, but our results suggest that some may play important roles in the brain's controllability even in underdeveloped connectomes. At the network level, our results suggest that nodes in more modular and topologically fragile networks are self-controlled under higher feedback costs, whereas those in more resilient networks are selfcontrolled under lower feedback. Although modularity is a

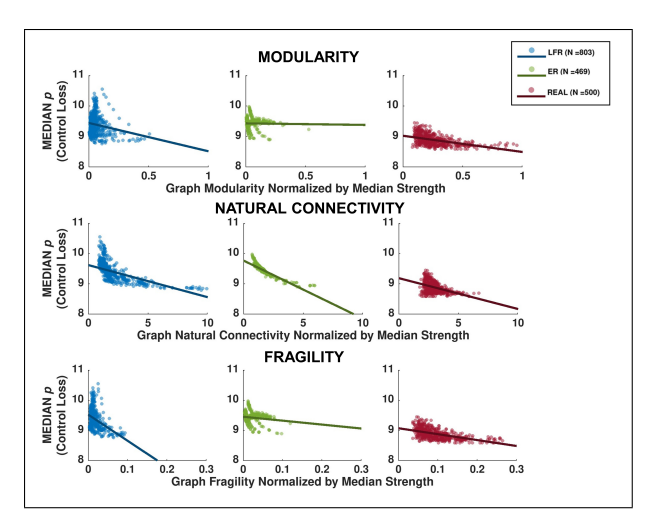


Fig. 5. Association between graph properties and median feedback cost at which nodes lose their control action.

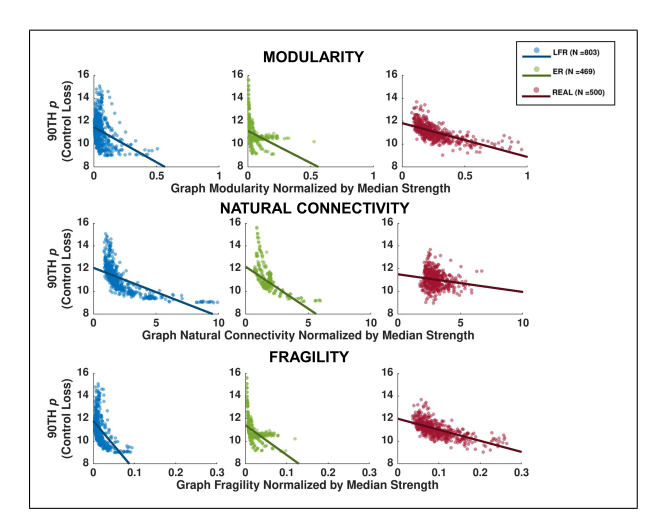


Fig. 6. Association between graph properties and 90^{th} percentile of feedback costs where nodes lose their control action.

key aspect of optimally organized networks, a high number of partitions could increase fragility. Self-control of nodes in suboptimally modular and fragile networks may then require higher feedback costs, whereas the opposite occurs in more resilient networks. This difference could be attributed to the tradeoff between control performance and cost, which is considered in the controller design problem. Thus, for a fragile network, a high feedback cost may be necessary to balance the controller's performance. At high feedback cost regimes, i.e., when nodes start losing their control action over the network, higher costs associated with this transition were correlated with lower modularity and fragility, i.e., were in the opposite direction than correlations associated with self-control, and low resilience. Some of these relationships were nonlinear, with feedback costs decreasing rapidly at low modularity, resilience, and fragility and changing very slowly thereafter. It is possible that when only a few nodes maintain their control action the associated feedback costs are invariant to at least some network properties. Our findings, suggest that the connectome's controllability at different

ranges of feedback costs may depend on regional topological properties, but less on the overall network topology, at least under very high feedback costs.

REFERENCES

- O. Sporns, DR. Chialvo, M. Kaiser, et al., Organization, Development and Function of Complex Brain Networks. Trends Cogn Sci., 2004, 8(9): 418-425.
- [2] C.J. Honey, R. Kötter, M. Breakspear, et al., Network Structure of Cerebral Cortex Shapes Functional Connectivity on Multiple Time Scales. Proc. Natl. Acad. Sci., 2007, 104 (24): 10240–45.
- [3] M.P. Van den Heuvel, O. Sporns, Network hubs in the human brain. Trends Cogn. Sci., 2013, 17(12):683-96.
- [4] K. Supekar, M. Musen, V. Menon, Development of large-scale functional brain networks in children. PLOS Biol., 2009, 7(7):e1000157.
- [5] D.A. Fair, A.L. Cohen, J.D. Power, et al., Functional brain networks develop from a "local to distributed" organization. PLOS Comput. Biol., 2009, 5(5):e1000381.
- [6] J.D. Power, D.A. Fair, B.L. Schlaggar, et al., The Development of Human Functional Brain Networks. Neuron, 2010, 67(5):735-748.
- [7] T.J. Whitford, C.J. Rennie CJ, S.M. Grieve SM, et al., Brain maturation in adolescence: concurrent changes in neuroanatomy and neurophysiology. Hum. Brain Mapp., 2007, 28:228–237.
- [8] Rempe MP, Ott LR, Picci G, et al., Spontaneous cortical dynamics from the first years to the golden years. Proc. Natl. Acad. Sci. USA, 2023, 120:e2212776120.
- [9] S. Gu, F. Pasqualetti, M. Cieslak, et al., Controllability of structural brain networks. Nat. Commun., 2015, 6:8414.
- [10] E.Tang, C. Giusti, G.L. Baum, et al., Developmental increases in white matter network controllability support a growing diversity of brain dynamics. Nat. Commun., 2017, 8:1252.
- [11] E. Wu-Yan, R.F. Betzel, E. Tang, et al., Benchmarking Measures of Network Controllability on Canonical Graph Models. J. Nonlinear Sci., 2020, 30: 2195–2233.
- [12] Q. Li, L. Yao, W. You, et al., Controllability of Functional Brain Networks and Its Clinical Significance in First-Episode Schizophrenia. Schizophr. Bull., 2023, 49(3):659–668.
- [13] J. Jeganathan, A., Perry, D.S. Bassett et al., Fronto-limbic dysconnectivity leads to impaired brain network controllability in young people with bipolar disorder and those at high genetic risk. Neuroimage Clin., 2018, 19:71-81.
- [14] H.B. Scheid, A. Ashourvan, J. Stiso, et al., Time-evolving controllability of effective connectivity networks during seizure progression. Proc. Natl. Acad. Sci. USA, 2021, 118(5):e2006436118.
- [15] M.I. Jordan, Computational aspects of motor control and motor learning. Handbook of Perception and Action, 1996, 2(2): 71-120.
- [16] M.T. deBettencourt MT, J.D. Cohen R.F. Lee et al., Closed-loop training of attention with real-time brain imaging. Nat. Neurosci., 2015, 18(3):470-5.
- [17] C. Zrenner, P. Belardinelli, F. Müller-Dahlhaus et al., Closed-Loop Neuroscience and Non-Invasive Brain Stimulation: A Tale of Two Loops. Front. Cell. Neurosci., 2016, 10:92.
- [18] R. Sitaram, T. Ros, L. Stoeckel et al., Closed-loop brain training: the science of neurofeedback. Nat. Rev. Neurosci., 2017, 18(2):86-100.
- [19] B.J. Casey, T. Cannonier, M.I. Conley, et al., The Adolescent Brain Cognitive Development (ABCD) study: Imaging acquisition across 21 sites. Developmental Cognitive Neuroscience, 2018, 32: 43-54.
- [20] Next-Generation-Neural-Data-Analysis: https://github.com/cstamoulis1/Next-Generation-Neural-Data-Analysis-NGNDA-
- [21] S.J Brooks, S.M Parks, C. Stamoulis, Widespread Positive Direct and Indirect Effects of Regular Physical Activity on the Developing Functional Connectome in Early Adolescence. Cereb. Cortex, 2021, 31(10):4840–4852
- [22] A. Lancichinetti, S. Fortunato, F. Radicchi, Benchmark graphs for testing community detection algorithms. Phys. Rev. E, 2008, 78(4):046110.
- [23] I. Mitrai, V.O. Jones, H. Dewantoro, et al., Internal control of brain networks via sparse feedback. AIChE J., 2023, 69(4):e18061.
- [24] F. Pasqualetti, S. Zhao, C. Favaretto, et al., Fragility Limits Performance in Complex Networks. Sci. Rep., 2020, 10:1774.
- [25] J. Wu, M. Barahona, Y.-J. Tan, et al., Natural Connectivity of Complex Networks. Chinese Phys. Lett., 2010, 27:078902